Determination of rate parameters of
cyclohexane and 1-hexene decomposition reactions

I. Gy. Zsély[a], T. Varga[a], T. Nagy[a], M. Cserháti[a], T. Turányi[a,*],

S. Peukert[b], M. Braun-Unkhoff[b], C. Naumann[b], U. Riedel[b]

[a] Institute of Chemistry, Eötvös University (ELTE), H-1117 Budapest, Pázmány P. sétány 1/A, Hungary

[b] Institute of Combustion Technology, German Aerospace Center (DLR), Pfaffenwaldring 38-40,

70569 Stuttgart, Germany

ABSTRACT

Peukert *et al.* recently published (*Int. J. Chem. Kinet.* 2010; 43: 107-119) the results of a series of shock tube measurements on the thermal decomposition of cyclohexane (c-C_6H_{12}) and 1-hexene (1-C_6H_{12}). The experimental data included 16 and 23 series, respectively, of H-atom profiles measured behind reflected shock waves by applying the ARAS technique (temperature range 1250–1550 K, pressure range 1.48–2.13 bar). Sensitivity analysis carried out at the experimental conditions revealed that the rate coefficients of the following six reactions have a high influence on the simulated H-atom profiles: R1: c-C_6H_{12} = 1-C_6H_{12}, R2: 1-C_6H_{12} = $C_3H_5 + C_3H_7$, R4: C_3H_5 = $aC_3H_4 + H$; R5: $C_3H_7 = C_2H_4 + CH_3$; R6: $C_3H_7 = C_3H_6 + H$; R8: $C_3H_5 + H = C_3H_6$. The measured data of Peukert *et al.* were re-analysed together with the measurement results of Fernandes *et al.* (*J. Phys. Chem. A* 2005; 109: 1063-1070) for the rate coefficient of reaction R4, the decomposition of allyl radicals. The optimization resulted in the following Arrhenius parameters: R1: A= 2.441×10^{19}, E/R= 52820; R2: A= 3.539×10^{18}, E/R= 42499; R4: A= 8.563×10^{19}, n= -3.665, E/R= 13825 (high pressure limit); R4: A= 7.676×10^{31} n= -3.120, E/R= 40323 (low pressure limit); R5: A= 3.600×10^{12}, E/R= 10699; R6: A= 1.248×10^{17}, E/R= 28538; R8: A= $6,212 \times 10^{13}$, E/R= -970. The rate parameters above are in cm^3, mol, s, and K units. Data analysis resulted in the covariance matrix of all these parameters. The standard deviations of the rate coefficients were converted to temperature dependent uncertainty parameter $f(T)$. These uncertainty parameters were typically f= 0.1 for reaction R1, f= 0.1–0.3 for reaction R2, below 0.5 for reaction R8 in the temperature range of 1250–1380K, and above 1 for reactions R4, R5, and R6.

---

[*] Corresponding author. Tel: +36 1 3722500, fax: +36 1 3722592.
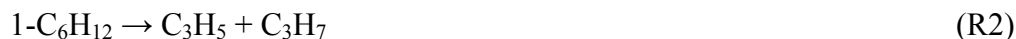*E-mail address:* turanyi@chem.elte.hu (Tamás Turányi).

Highlights

- Recent experimental data obtained in shock tube measurements by Peukert *et al.* (2010) and Fernandes *et al.* (2005) were re-analysed.
- Arrhenius parameters belonging to six important reactions of transportation fuel combustion were determined.
- The data analysis provided the covariance matrix of the Arrhenius parameters and the uncertainty parameter – temperature functions of the rate coefficients.

1. Introduction

Practical transportation fuels (*e.g.* diesel, kerosene) contain a large number of species (up to several thousands) [1]; consequently, it is not possible to develop detailed chemical kinetic mechanisms describing the combustion in detail for all these fuel molecules. Surrogate fuel mixtures are defined in such a way that these mixtures well reproduce the major chemical properties (*e.g.* ignition time, flame velocity) [2] and/or the physical properties (*e.g.* viscosity, vapour pressure) of real fuels. Surrogate fuels with well defined composition are also needed to make the engine experiments reproducible. Surrogate fuel mixtures often include cyclohexane and 1-hexene, as representatives of cycloalkanes and alkenes [3].

The thermal decomposition of cyclohexane gives solely 1-hexene, while the decomposition of 1-hexene yields allyl and *n*-propyl radicals

$$\text{c-C}_6\text{H}_{12} \rightarrow \text{1-C}_6\text{H}_{12} \tag{R1}$$

$$\text{1-C}_6\text{H}_{12} \rightarrow \text{C}_3\text{H}_5 + \text{C}_3\text{H}_7 \tag{R2}$$

These two reactions are important steps of the combustion mechanism of surrogate fuels containing cyclohexane and 1-hexene.

Recently, Peukert *et al.* [4] investigated experimentally the formation of H-atoms in the pyrolysis of cyclohexane and 1-hexene by applying the shock tube technique combined with the ARAS-technique (atomic resonance absorption spectroscopy). They proposed a detailed chemical kinetic reaction model for reproducing the measured H-atom absorption profiles. One of the major steps of their reaction model is the decomposition of the allyl radical to allene and hydrogen atom:

$$\text{C}_3\text{H}_5 = \text{aC}_3\text{H}_4 + \text{H} \tag{R4}$$

The numbering of the reactions in this article is in accordance with that of the paper of Peukert *et al.* [4]. Reaction R4 had been investigated by Fernandes *et al.* [5] by shock tube experiments coupled with H-ARAS as detection method. They performed a series of experiments for pressures near 0.25, 1, and 4 bar using Ar and N_2 as bath gases. The experiments covered temperatures ranging from 1125 K up to 1570 K.

Turányi and co-workers recently suggested [6] a new approach for the determination of the rate parameters of kinetic reaction mechanisms, by fitting several rate parameters simultaneously to a large amount of

experimental data. This method was used in the present work to extract more information from the experimental data of Peukert *et al.* [4] and Fernandes *et al.* [5].

The methodology used here has some similarities with that of Sheen and Wang [7]. These authors investigated n-heptane combustion by evaluating multispecies signals measured in shock tube experiments, together with the results of other indirect measurements, like laminar flame velocity and ignition delay time. There are, however, significant differences between the two methods. For example, Sheen and Wang optimized *A*-factors only and did not utilize the results of direct measurements.

According to our procedure, rate parameters were obtained for several elementary reactions of the cyclohexane and 1-hexene thermal decomposition reaction systems. We have exploited the good feature of our method that experimental data of very different types can be interpreted simultaneously. The obtained rate parameters have not been determined previously in this temperature and pressure range. Also, the analysis resulted in a detailed characterization of the correlated uncertainty of all obtained Arrhenius parameters.

2. Overview of the experimental results

Peukert *et al.* [4] investigated the decomposition of cyclohexane (c-C_6H_{12}) and 1-hexene (1-C_6H_{12}) in shock tube experiments. Gas mixtures of $1.1 - 2.0$ ppm cyclohexane and $1.0 - 2.4$ ppm 1-hexene, respectively, diluted with Ar were used. Time-resolved H-atom absorption − time profiles were measured behind reflected shock waves. For cyclohexane, 16 H-profiles were collected over a temperature range of 1305–1554 K at pressures ranging from 1.68 to 2.13 bar. The 23 H-atom profiles obtained from the 1-hexene experiments were measured at temperatures between 1253 and 1398 K and pressures between 1.48 and 2.02 bar. Peukert *et al.* recommended a 13-step reaction model, which is listed in Table 1. They stated that this mechanism is sufficient for the interpretation of their cyclohexane and 1-hexene experimental results.

Peukert *et al.* assigned the rate parameters of all reactions, besides those of reaction R2, to the best available literature values. These Arrhenius parameters, together with their references, are given in Table 1. Peukert *et al.* fitted the rate coefficient of reaction R2 in each 1-hexene experiment separately, till the best reproduction of the H-atom profile. In the next step, the temperature − rate coefficient data pairs were used to obtain Arrhenius parameters *A* and *E*. These Arrhenius parameters for reaction R2 are also given in Table 1. The cyclohexane decomposition measurements have not been used for fitting the Arrhenius parameters of reaction R1, because the measured H-profiles of the cyclohexane series could be reproduced by using the rate parameters suggested by Tsang [8]; for details see Peukert *et al.* [4].

According to their analysis, the formation of H-atoms observed in these shock tube experiments is almost entirely a result of the dissociation of allyl radicals to allene and H-atoms (R4); therefore the rate coefficient of this reaction is assumed to be of dominant importance for the interpretation of the experiments. Fernandes *et al.* [5] recently measured the rate coefficient of this reaction and derived three Arrhenius expressions, recommended for pressures 0.25 bar, 1 bar, and 4 bar. Unfortunately, these pressures are not very close to the pressures of the Peukert *et al.* experiments (1.48 – 2.13 bar). Peukert *et al.* used [4] the following reasoning: „Our experiments were carried out at pressures around 2 bar. The rate coefficient values of the 1 and 4 bar experiments approximately differ by a factor of 2. Therefore, we used the rate coefficient expression for 1 bar and increased the pre-exponential factor *A* by 1.6". The Arrhenius parameters they used, attributed to 2 bar, are given in Table 1. The drawback of the application of a single Arrhenius expression valid at 2 bar is that in the Peukert's experiments the pressure was varied between 1.48 and 2.13 bar.

As a first step of the re-analysis of the data, all experimental data files were converted to the PrIMe format [9]. This is an XML data format that was designed to be a universally applicable definition of combustion related experiments. Then, the Matlab utility code of Varga *et al.* [10] was used. This program is able to read and interpret PrIMe datafiles, invoke the corresponding simulation code of CHEMKIN-II [11] or Cantera [12], and present the results. In this case, the SENKIN simulation code [13] was used for the calculation of concentration profiles. The sensitivities were determined using a brute force method by multiplying the *A* factors with 0.5 and calculating the local sensitivity coefficients by finite difference approximation. The calculation of the sensitivity coefficients was repeated with multiplication factors 1.01 and 1.5, and the calculated sensitivity results were very similar. To get a comprehensive picture, the maximum of the absolute sensitivity value was taken for each reaction and all sensitivity coefficients were normalized to the largest one in each experiment. The results of the sensitivity analysis are presented in Table 2.

According to this sensitivity analysis, the calculated H-atom concentrations were sensitive to the rate coefficients of the following six reactions: R1: $c\text{-}C_6H_{12}=1\text{-}C_6H_{12}$; R2: $1\text{-}C_6H_{12} = C_3H_5 + C_3H_7$; R4: $C_3H_5 = C_3H_4 + H$; R5: $C_3H_7 = C_2H_4 + CH_3$; R6: $C_3H_7 = C_3H_6 + H$; R8: $C_3H_5 + H = C_3H_6$. For the cyclohexane decomposition experiments, the most sensitive reactions were R1, R2, and R4 – R6; while for the 1-hexene decomposition experiments, the most sensitive reactions were R2, R4 – R6, and R8.

Fernandes *et al.* [5] listed the measured k_{uni} rate coefficients, belonging to various pressures (0.28 – 0.38 bar, 1.23 – 1.29 bar, and 4.21 – 4.56 bar) and temperatures (1123 K – 1567 K). They interpreted these experimental data on the basis of the RRKM theory.

In the present work, we have fitted the experimentally determined k_{uni} rate coefficients (40 values) of Fernandes *et al.* using the Lindemann scheme (see e.g. [14], and the SENKIN manual [13]). The fitting resulted in the following rate parameters for reaction R4: high pressure limit $A = 9.759 \times 10^{16}$, $n = -2.826$, $E/R = 12{,}670$; low pressure limit $A = 2.0390 \times 10^{35}$, $n = -4.180$, $E/R = 40926$; the units are cm^3, s, and K. The average root-

mean-square error of the fit was 18.86 %. We also tried to approximate the k_{uni} values by not only the high and low pressure Arrhenius parameters, but also a temperature independent F_{cent} parameter. Using this 7-parameter description instead of the 6-parameter (Lindemann) parameterization did not decrease significantly the root-mean-square error. Therefore, we concluded that the 6-parameter Lindemann scheme is sufficient for the approximation of the experimental k_{uni} values of Fernandes *et al.*.

In order to enlarge the experimental data basis, a literature survey was carried out to find more direct measurements to the reactions listed in Table 1. Unfortunately, very few direct measurements have been published for these reactions [15-24]. In principle, in these experiments the elementary reactions were investigated in a very different range of temperature and pressure. Typically, if the pressure was around 1 to 2 atm, then the temperature was much lower (500–900 K). Alternatively, the high temperature (900–2000 K) experiments were associated with very low pressure, usually below 5 Torr. Therefore, it was not possible to include further experimental data in our analysis.

3. Methods of kinetic parameter estimation

The new method recently suggested by Turányi *et al.* [6] has the following features:

(i)   Direct and indirect measurements are considered simultaneously. In the direct kinetic measurements, the rate parameters of a single elementary reaction step are determined. In the recent publications, the measured rate coefficients are listed together with the experimental conditions (*e.g.* temperature, pressure, bath gas). The results of indirect experiments can be interpreted only via simulations using a complex reaction mechanism. Examples for indirect measurement data are concentration profiles determined in a shock tube or tubular reactor, or measured laminar flame velocities.

(ii)   The sensitivities of the simulated values corresponding to the measured signal in the indirect experiments with respect to the rate parameters are calculated. This sensitivity analysis is used for the identification of the rate parameters to be optimized. Experimental rate coefficients determined in direct experiments belonging to the highly sensitive reactions are collected.

(iii)   The domain of uncertainty of the rate parameters is determined on the basis of a literature review.

(iv)   The optimized values of the rate parameters of the selected elementary reactions within their domain of uncertainty are determined using a global nonlinear fitting procedure.

The following objective function is used in our calculations:

$$E(\mathbf{p}) = \sum_{i=1}^{N} E_i(\mathbf{p}) = \sum_{i=1}^{N} \frac{w_i}{N_i} \sum_{j=1}^{N_i} \left(\frac{Y_{ij}^{\mathrm{mod}}(\mathbf{p}) - Y_{ij}^{\mathrm{exp}}}{\sigma(Y_{ij}^{\mathrm{exp}})} \right)^2 ,$$

$$\text{where } Y_{ij} = \begin{cases} y_{ij} & \text{if } \sigma(y_{ij}^{\mathrm{exp}}) \approx \text{constant} \\ \ln y_{ij} & \text{if } \sigma(\ln y_{ij}^{\mathrm{exp}}) \approx \text{constant} \end{cases},$$

(1)

where $\mathbf{p} = (p_1, p_2, \ldots, p_{n_p})$ is the vector of parameters. Parameter vector $\mathbf{p}$ includes the Arrhenius parameters of the selected reactions and it may contain other rate parameters such as branching ratios, third body efficiencies, parameters describing the pressure dependence (*e.g.* Troe or SRI parameters), thermodynamic data, *etc.*. The published results of direct measurements include rate coefficients k measured at given conditions (*e.g.* temperature, pressure, and bath gas). In the case of indirect measurements, the results are data such as ignition delay times and/or laminar flame velocities. In equation (1), N is the number of measurement series (direct and indirect together), and N_i is the number of data points in the ith measurement series. Value y_{ij}^{exp} is the jth data point in the ith measurement series. The corresponding modeled value $y_{ij}^{\mathrm{mod}}(\mathbf{p})$ for parameter set $\mathbf{p}$ can be obtained by calculating the rate coefficient at the given temperature (and pressure, bath gas etc.), or by carrying out a simulation with combustion kinetic codes using an appropriate detailed mechanism.

The form of the objective function includes automatic weighting according to the number of data points and the standard deviation of the data $\sigma(Y_{ij}^{\mathrm{exp}})$. Additional individual weighing w_i of the ith measurement series can also be taken into account according to the consideration of the user. Users of the method might want to emphasize some measurements or decrease the weight of others.

The objective function can be transformed into a simpler form by introducing a single index k which runs through all data points of all measurement series. A new unified weight $\mu_k = w_k/N_k$ is used for each data point, which further simplifies the objective function:

$$E(\mathbf{p}) = \sum_{k=1}^{N} \mu_k \left(\frac{Y_k^{\mathrm{mod}}(\mathbf{p}) - Y_k^{\mathrm{exp}}}{\sigma(Y_k^{\mathrm{exp}})} \right)^2 .$$

(2)

This equation can be condensed by introducing matrix−vector notation:

$$E(\mathbf{p}) = \left(\mathbf{Y}_{\mathrm{mod}}(\mathbf{p}) - \mathbf{Y}_{\mathrm{exp}} \right)^{\mathrm{T}} \mathbf{W} \mathbf{\Sigma}_{\mathbf{Y}}^{-1} \left(\mathbf{Y}_{\mathrm{mod}}(\mathbf{p}) - \mathbf{Y}_{\mathrm{exp}} \right) .$$

(3)

Here $\mathbf{Y}_{\mathrm{mod}}(\mathbf{p})$ and $\mathbf{Y}_{\mathrm{exp}}$ denote the column vectors formed from values of $Y_k^{\mathrm{mod}}(\mathbf{p})$ and Y_k^{exp}.

$$\mathbf{Y}_{\mathrm{mod}}(\mathbf{p}) = \left(Y_1^{\mathrm{mod}}(\mathbf{p}) \quad \ldots \quad Y_N^{\mathrm{mod}}(\mathbf{p}) \right)^{\mathrm{T}}, \qquad \mathbf{Y}_{\mathrm{exp}} = \left(Y_1^{\mathrm{exp}} \quad \ldots \quad Y_N^{\mathrm{exp}} \right)^{\mathrm{T}} .$$

(4)

Matrices $\mathbf{W}$ and $\mathbf{\Sigma}_{\mathbf{Y}}$ are the diagonal matrices of weights μ_k and variances $\sigma^2(Y_k^{\mathrm{exp}})$.

The covariance matrix of the fitted parameters $\mathbf{\Sigma}_{\mathbf{p}}$ was estimated using the following equation:

$$\Sigma_{\mathbf{p}} = \left[\left(\mathbf{J}_{o}^{\mathrm{T}} \mathbf{W} \Sigma_{\mathbf{Y}}^{-1} \mathbf{J}_{o} \right)^{-1} \mathbf{J}_{o}^{\mathrm{T}} \mathbf{W} \Sigma_{\mathbf{Y}}^{-1} \right] \left(\Sigma_{\mathbf{Y}} + \Sigma_{\Delta} \right) \left[\left(\mathbf{J}_{o}^{\mathrm{T}} \mathbf{W} \Sigma_{\mathbf{Y}}^{-1} \mathbf{J}_{o} \right)^{-1} \mathbf{J}_{o}^{\mathrm{T}} \mathbf{W} \Sigma_{\mathbf{Y}}^{-1} \right]^{\mathrm{T}}, \tag{5}$$

where $\Sigma_{\Delta} \approx \Delta \mathbf{Y} \Delta \mathbf{Y}^{\mathrm{T}}$, $\Delta \mathbf{Y} \approx \overline{\mathbf{Y}}_{\mathrm{mod}} - \mathbf{Y}_{\mathrm{exp}}$. This equation has been derived in ref. [6]. Here $\mathbf{J}_0$ is the derivative matrix of $\mathbf{Y}_{\mathrm{mod}}$ with respect to $\mathbf{p}$ at the optimum.

The diagonal elements of matrix $\Sigma_{\mathbf{p}}$ are the variances of parameters $\sigma^2(p_i)$. The off-diagonal elements are covariances $\mathrm{cov}(p_i, p_j) = r_{p_i, p_j} \sigma_{p_i} \sigma_{p_j}$, therefore the correlation coefficients r_{p_i, p_j} can be calculated from the off-diagonal element and the standard deviations:

$$r_{p_i, p_j} = \frac{(\Sigma_{\mathbf{p}})_{i,j}}{\sigma_{p_i} \sigma_{p_j}}. \tag{6}$$

Covariances of the logarithm of the rate coefficients at temperature T can be calculated [6] in the following way:

$$\mathrm{cov}\left(\ln k_i(T), \ln k_j(T)\right) = \mathbf{\Theta}^{\mathrm{T}} \Sigma_{\mathbf{p}_i, \mathbf{p}_j} \mathbf{\Theta}. \tag{7}$$

Here $\mathbf{\Theta} := (1, \ln\{T\}, -T^{-1})^{\mathrm{T}}$, $\mathbf{p}_i := (\ln A_i, n_i, \mathrm{E}_i/R)^{\mathrm{T}}$, and $\Sigma_{\mathbf{p}_i, \mathbf{p}_j}$ denotes a block of matrix $\Sigma_{\mathbf{p}}$ that contains the covariances of the Arrhenius parameters of reactions i and j. Equation (7) provides variance $\sigma^2(\ln k_i(T))$ if $i = j$.

In high-temperature gas kinetics, the uncertainty of the rate coefficient at given temperature T is usually defined by uncertainty parameter f in the following way:

$$f(T) = \log_{10}\left(k^0(T)/k^{\min}(T)\right) = \log_{10}\left(k^{\max}(T)/k^0(T)\right), \tag{8}$$

where k^0 is the recommended value of the rate coefficient and values below $k^{\min}$ and above $k^{\max}$ are considered to be very improbable. Assuming that the minimum and maximum values of the rate coefficients correspond to 3σ deviations from the recommended values on a logarithmic scale, uncertainty f can be obtained [25] at a given temperature T from the standard deviation of the logarithm of the rate coefficient using the following equation:

$$f(T) = 3\,\sigma(\log_{10} k) = \frac{3}{\ln 10}\,\sigma(\ln k). \tag{9}$$

Using $\sigma(\ln k)$ calculated by equation (7), the $f(T)$ function obtained has a statistical background and it is deduced from experimental data.

4. Estimation of rate parameters based on all experimental data

Application of objective function (1) requires the estimation of the variance of the data points. In our calculations, 7-16 % relative standard deviation was assumed for the data points of the 1-hexene experiments [4], 6-56 % for the data points of the cyclohexane experiments [4]. These standard deviation values were different for each measurement; they were determined from the scatter of the measured H-atom concentrations. The individual standard deviation belonging to each experimental data set is given in the last column of Table 2. For the experiments of Fernandes *et al.* [5], 20% relative standard deviation was assumed based on the scatter of the data, which is in good accordance with the error of the Lindemann fitting.

The process of parameter optimization can be followed in Table 3. The reaction model of Peukert *et al.*, using their rate parameters is given in the 3rd column of Table 1. Using these rate parameters, the 1-hexene experiments are well described (the objective function value is 118). The agreement of the modelled results with the experimental data can be characterized by the value of the objective function (1). For the cyclohexane experimental data, the agreement is also good (objective function value 463); the model also performed well when both experimental datasets − 1-hexene and cyclohexane − were included in the objective function (581). As the reaction model of Peukert *et al.* includes a single Arrhenius expression for reaction R4, attributed to pressure 2 bar, of course their reaction model can be used neither for the description of the Fernandes experiments, nor for the cases when the two types of experimental data are considered together.

The initial mechanism of our optimization is identical to the published Peukert mechanism, except for the rate parameters of reaction R4 and R8. For reaction R8, an equivalent two parameter Arrhenius was used instead of the original three parameter expression ($A= 2.345\times10^{14}$, $E/R= 193.26$). In our initial mechanism, the Lindemann expression was used for the description of reaction R4 based on the Fernandes data only (for the values of the Arrhenius parameters see above). These rate parameters result in a very good description of the Fernandes' experiments (objective function value 9), but spoiled the agreement with all the Peukert experimental data (the objective function value is 878).

Therefore, the initial mechanism was improved by fitting the Arrhenius parameters of all the highly sensitive reactions, which means 16 Arrhenius parameters in total. This seems to be a large number of simultaneously fitted parameters, but the fitting is based on also a large number of experimental data. The Peukert *et al.* experiments contain 39 concentration profiles with 1000 data points each (39000 data points). The Fernandes *et al.* experiments provided additional 40 data points for the determination of the temperature and pressure dependence of reaction R4. The number of datasets, N, was 40. If all data series had equal weight, it would have resulted in the Fernandes' data very little (1/40) contribution. Therefore, $w_i = 10$ weighting was used for the Fernandes *et al.* data series, which increased its contribution to about one fifth.

In the optimization, all cyclohexane and 1-hexene measurements of Peukert *et al.* [4] and the experiments of Fernandes *et al.* [5] were considered. In a Monte Carlo sampling, the Arrhenius parameters of five sensitive reactions (R2, R4 – R6, and R8) were varied independently in such a way that all rate coefficients changed ± one magnitude. 250 parameter sets were generated, the objective function was evaluated for each parameter set, and the best parameter set was selected. Starting from this parameter set, in fifty iteration cycles the parameter space was explored in narrower regions in a similar way and the best parameter set was accepted as the final one. As a result of the optimization, the reproduction of the Peukert *et al.* data improved dramatically (the value of the objective function decreased from 878 to 482), while the agreement with the Fernandes *et al.* experimental data remained good (9 to 10). The obtained optimized Arrhenius parameters are given in Table 1.

As Table 3 shows, using all available experimental data for the optimization kept the good description of the 1-hexene measurements and the experiments of Fernandes et al. [5], while at the same time, it improved the description of the cyclohexane experiments. As examples, Figures 1 and 2 show the data points belonging to one 1-hexene and one cyclohexane experiments, respectively. Each figure presents two simulated concentration curves, one calculated with the initial mechanism and another one using the final parameter set. Figure 3 presents the results of the Fernandes *et al.* experiments and the calculated k_{uni} values, when the rate parameters of the Lindemann scheme are fitted to the Fernandes' experimental data points and the k_{uni} values calculated from the rate parameters of reaction R4 of the final parameter set.

Figure 4 shows the temperature dependence of the rate coefficients of the investigated reactions in Arrhenius plots. It is clear that the optimization changed the rate coefficient–temperature functions of all reactions and not only shifted the lines, but changed their slope, too.

Using equations (5) and (6) the covariance and correlation matrices, respectively, were calculated in the optimum. Tables S1 and S2 of the Electronic Supplement present these matrices. It is not easy to overview the covariance matrix, but this is the information that should be used in a detailed uncertainty analysis, that takes into account also the correlation of the rate parameters. The correlation matrix shows that there is a high correlation between all parameters. Not only the *A − E/R* parameter pairs are highly correlated, but also each other pairs of parameters.

The traditional characterization of the uncertainty of the rate coefficients using equation (8) is not informative enough, because it describes the uncertainty of each rate coefficient separately. However, the chemical kinetic databases use this type of uncertainty characterization. Therefore, we also calculated the temperature dependent uncertainty parameters from the standard deviations of the logarithm of the rate coefficients using equation (9). Figure 5 shows that reaction R1 has extremely low uncertainty; the uncertainty parameter is temperature dependent and it has a minimum near 1430 K. The value of the uncertainty parameter is around 0.1, which means that the corresponding rate coefficient is well known. Reactions R2 and R8 have

middle level uncertainty ($f = 0.1–0.3$ for reaction R2, below 0.5 for reaction R8 in the temperature range of 1250–1380K). The uncertainty of the other determined rate coefficients is quite large, above 1.

5. Conclusions

The experimental data such as concentration profiles obtained in shock tube experiments are usually interpreted by using a detailed reaction mechanism. The rate parameters of all reactions but one are assigned to literature values and the rate parameters of a single reaction are fitted to reproduce the experimental data. The requirements for the selection of this reaction step is that the simulated signal at the conditions of the experiments should be very sensitive to the corresponding rate parameters, and also, these rate parameters should be the least known (most uncertain) from all the highly sensitive parameters.

In the present paper, an alternative approach was used which is generally applicable for the interpretation of indirect measurements. The most sensitive reactions are identified at the experimental conditions. Results of direct measurements (measured rate coefficients at various temperatures and pressures) belonging to the highly sensitive reactions are collected. The rate parameters of all highly sensitive reactions are fitted simultaneously to all available (direct and indirect) experimental data. This parameter optimization is possible, if the objective function handles all available experimental data in a similar way and if the fitting procedure explores the whole physically realistic domain of the rate parameters. The great advantage of this approach is that the determined parameters depend very little on the assumed values of the not fitted rate parameters.

In this article, this approach was demonstrated on the re-evaluation of the 1-hexene pyrolysis measurements (23 data sets) and the cyclohexane pyrolysis measurements (16 data sets) of Peukert *et al.* [4]. The direct measurements of Fernandes *et al.* [5] for the determination of the temperature and pressure dependence of the rate coefficient of the decomposition reaction of the allyl radical to allene and hydrogen atom (R4) were also taken into account. In total, 16 rate parameters of the following six reaction steps were determined: R1: $c\text{-}C_6H_{12}$ = $1\text{-}C_6H_{12}$, R2: $1\text{-}C_6H_{12}$ = $C_3H_5 + C_3H_7$, R4: C_3H_5 = $aC_3H_4 + H$, R5: C_3H_7 = $C_2H_4 + CH_3$, R6: C_3H_7 = $C_3H_6 + H$, R8: $C_3H_5 + H$ = C_3H_6. The uncertainty parameters were typically $f = 0.1$ for reaction R1, $f = 0.1–0.3$ for reaction R2, below 0.5 for reaction R8 in the temperature range of 1250–1380K, and above 1 for reactions R4, R5, and R6. This means that the newly determined rate parameters are reliable for reactions R1 and R2. It is acceptable for reaction R8 at temperatures near 1300 K and pressures above 1 atm. The new rate coefficients for the other reactions are the best fit for these experiments, but due to their large f uncertainty parameters they cannot be considered as new recommendations. The statistical based, temperature dependent characterization of the uncertainty of the rate parameters is a novelty of our approach. Except for reaction R4, the rate parameters of

these reactions have not been measured in the temperature range 1250–1550 K and pressure range 1.48–2.13 bar. This temperature and pressure region is close to the one of the practical combustion applications.

Acknowledgements

References

[1] Dagaut P, El Bakali A, Ristori A. The combustion of kerosene: experimental results and kinetic modeling using 1- to 3-components surrogate model fuels. Fuel 2006;85:944-56.

[2] Dagaut P, Gaïl S. Kinetics of gas turbine liquid fuels combustion: Jet-A1 and bio-kerosene. ASME Turbo Expo 2007: Power for Land, Sea, and Air 2007;GT2007-27145:93-101.

[3] Colket M, Edwards T, Williams S, Cernansky NP, Miller DL, Egolfopoulos F, et al. Development of an experimental database and kinetic models for surrogate jet fuels. 45th AIAA Aerospace Sciences Meeting and Exhibit, Reno NV, January 8-11, 2007 AIAA Paper: 2007-770 2007.

[4] Peukert S, Naumann C, Braun-Unkhoff M, Riedel U. Formation of H-atoms in the pyrolysis of cyclohexane and 1-hexene: A shock tube and modeling study. International Journal of Chemical Kinetics 2010;43:107-19.

[5] Fernandes R, Raj Giri B, Hippler H, Kachiani C, Striebel F. Shock wave study on the thermal unimolecular decomposition of allyl radicals. Journal of Physical Chemistry A. 2005;109:1063-70.

[6] Turányi T, Nagy T, Zsély IG, Cserháti M, Varga T, Szabó B, et al. Determination of rate parameters based on both direct and indirect measurements. International Journal of Chemical Kinetics 2011:submitted.

[7] Sheen D, Wang H. Combustion kinetic modeling using multispecies time histories in shock-tube oxidation of heptane. Combust Flame 2011;158:645-56.

[8] Tsang W. Thermal stability of cyclohexane and 1- hexene. International Journal of Chemical Kinetics 1978;10:1119-38.

[9] Frenklach M. PrIMe Database, http://wwwprimekineticsorg/.

[10] Varga T, Zsély IG, Turányi T. Collaborative development of reaction mechanisms using PrIMe data files. Proceedings of the European Combustion Meeting 2011. Paper 164.

[11] Kee RJ, Rupley FM, Miller JA. CHEMKIN-II: A FORTRAN Chemical kinetics package for the analysis of gas-phase chemical kinetics. Sandia National Laboratories; 1989.

[12] Cantera. An open-source, object-oriented software suite for combustion. http://sourceforgenet/projects/cantera/, http://codegooglecom/p/cantera/.

[13] Lutz AE, Kee RJ, Miller JA. Senkin: A Fortran program for predicting homogeneous gas phase chemical kinetics with sensitivity analysis. Sandia National Laboratories; 1988.

[14] Pilling MJ, Seakins PW. Reaction kinetics: Oxford University Press, 1995.

[15] Tsang W. Influence of local flame displacement velocity on turbulent burning velocity. International Journal of Chemical Kinetics 1978;10:1119-38.

[16] King KD. Very low-pressure pyrolysis (VLPP) of hex-1-ene. Kinetics of the retro-ene decomposition of a mono-olefin. International Journal of Chemical Kinetics 1979;11:1071-80.

[17] Brown TC, King KD, Nguyen TT. Kinetics of primary processes in the pyrolysis of cyclopentanes and cyclohexanes. Journal of Physical Chemistry 1986;90:419-24.

[18] Kiefer JH, Gupte KS, Harding LB, Klippenstein SJ. Shock Tube and theory investigation of cyclohexane and 1-hexene decomposition. Journal of Physical Chemistry A 2009;113:13570-85.

[19] Yamauchi N, Miyoshi A, Kosaka K, Koshi M, Matsui H. Thermal decomposition and isomerization processes of alkyl radicals. Journal of Physical Chemistry A 1999;103:2723-33.

[20] Hanning-Lee MA, Pilling MJ. Kinetics of the reaction between H atoms and allyl radicals. International Journal of Chemical Kinetics 1992;24:271-8.

[21] Camilleri P, Marshall RM, Purnell H. Arrhenius parameters for the unimolecular decomposition of azomethane and n-propyl and isopropyl radicals and for methyl attack on propane. Journal of Chemical Society, Faraday Transactions 1. 1975;71:1491.

[22] Mintz KJ, Le Roy DJ. Kinetics of radical reactions in sodium diffusion flames. Canadian Journal of Chemistry 1978;56(7):941-9.

[23] Lin MC, Laidler KJ. Kinetics of the decomposition of ethane and propane sensitized by azomethane. The decomposition of the normal propyl radical. Canadian Journal of Chemistry 1966;44:2927-40.

[24] Allara DL, Shaw R. A compilation of kinetic parameters for the thermal degradation of n-alkane molecules. J Phys Chem Ref Data 1980;9:523-60.

[25] Turányi T, Zalotai L, Dóbé S, Bérces T. Effect of the uncertainty of kinetic and thermodynamic data on methane flame simulation results Phys Chem Chem Phys 2002;4:2568-78.

[26] Yamauchi N, Miyoshi A, Kosaka K, Koshi M, H M. Thermal decomposition and isomerization processes of alkyl radicals. Journal of Physical Chemistry A 1999;103:2723-33.

[27] Tsang W. Chemical kinetic data base for combustion chemistry Part V. Propene. Journal of Physical and Chemical Reference Data 1991;20:221–73.

[28] Harding LB, Klippenstein SJ, Georgievskii Y. On the combination reactions of hydrogen atoms with resonance-stabilized hydrocarbon radicals. Journal of Physical Chemistry A 2007;111:3789-801.

[29] Kiefer JH, Kumaran SS, Mudipalli PS. The mutual isomerization of allene and propyne. Chemical Physics Letters. 1994;224:51-5.

[30] Bentz T. PhD Thesis Stoßwellenuntersuchungen zur Reaktionskinetik ungesättigter und teiloxidierter Kohlenwassestoffe. Karlsruhe: Universitat Karlsruhe, 2007.

[31] Bentz T, Giri B, Hippler H, Olzmann M, Striebel F, Szőri M. Reaction of hydrogen atoms with propyne at high temperatures: An experimental and theoretical study. Journal of Physical Chemistry A. 2007;111:3812-8.

Table 1

The mechanism used for the interpretation of the cyclohexane and 1-hexene pyrolysis experiments.

	Reaction	Arrhenius parameters used by Peukert *et al.* [4]				Optimized Arrhenius parameters (see text)		
		A	*n*	*E/R*	*Ref.*	*A*	*n*	*E/R*
R1	c-C_6H_{12} = l-C_6H_{12}	5.0×10^{16}	0	44483	[8]	2.441×10^{19}	0	52820
R2	1-C_6H_{12} = C_3H_5 + C_3H_7	2.3×10^{16}	0	36672	[4]	3.539×10^{18}	0	42499
R3	l-C_6H_{12} = $2C_3H_6$	4.0×10^{12}	0	28867	[8]	–	–	–
R4	C_3H_5 = aC_3H_4 + H *p*= 2 atm	8.5×10^{79}	-19.29	47979	[5] [a]	–	–	–
	C_3H_5 = aC_3H_4 + H high pressure limit	–	–	–		8.563×10^{19}	−3.665	13825
	C_3H_5 = aC_3H_4 + H low pressure limit	–	–	–		7.676×10^{31}	−3.120	40323
R5	C_3H_7 = C_2H_4 + CH_3	1.8×10^{14}	0	15751	[26]	3.600×10^{12}	0	10699
R6	C_3H_7 = C_3H_6 + H	6.9×10^{13}	0	18872	[26]	1.248×10^{17}	0	28538
R7	C_3H_5 + H = aC_3H_4 + H_2	1.8×10^{13}	0	0.0	[27]	–	–	–
R8	C_3H_5 + H = C_3H_6	5.3×10^{13}	0.18	-63	[28]	6.212×10^{13}	0	−970
R9	aC_3H_4 = pC_3H_4	1.1×10^{14}	0	32355	[29]	–	–	–
R10	aC_3H_4 + H→pC_3H_4 + H	4.0×10^{17}	0	2560	[30]	–	–	–
R-10	pC_3H_4 + H→aC_3H_4 + H	1.9×10^{14}	0	3090	[32]	–	–	–
R11	aC_3H_4 + H = C_3H_3 + H_2	4.0×10^{14}	0	7500	[30]	–	–	–
R12	pC_3H_4 + H = C_3H_3 + H_2	3.4×10^{14}	0	6290	[31]	–	–	–
R13	pC_3H_4 + H = C_2H_2 + CH_3	3.1×10^{14}	0	4010	[31]	–	–	–

Rate coefficients in the form $k(T) = A\,T^n \exp(-E_a/RT)$ in cm^3, mol, s, and K units.

[a] Pre-exponential factor *A* of the 1 bar expression of Fernandes *et al.* [5] has been increased by 1.6.

Table 2

The maximum values of the absolute sensitivities in the time domain 0–1.0 ms, normalized to the largest sensitivity value in each experiment. Sensitivities larger than 0.1 are indicated by bold. The last column shows the assumed relative standard deviation of the data points in each series of experiments. These values were used for the evaluation of objective function (1).

Filename	C6H12-c=1-C6H12	1-C6H12 = C3H5+C3H7	1-C6H12=2C3H6	C3H5 = C3H4 + H	C3H7 = C2H4 + CH3	C3H7 = C3H6 + H	C3H5 + H = C3H4 + H2	C3H5 + H = C3H6	C3H4 = PC3H4	C3H4+H=>PC3H4+H	PC3H4+H=>C3H4+H	C3H4+H => C3H3+H2	PC3H4+H => C3H3+H2	PC3H4 + H = C2H2 + CH3	% std. Deviation
	R1	**R2**	**R3**	**R4**	**R5**	**R6**	**R7**	**R8**	**R9**	**R10**	**R-10**	**R11**	**R12**	**R13**	
21	**0.50**	**0.50**	0.02	**0.40**	**1.00**	**0.50**	0.00	0.00	0.02	0.00	0.00	0.00	0.00	0.00	55.8
22	**0.52**	**0.52**	0.02	**0.40**	**1.00**	**0.52**	0.00	0.00	0.00	0.00	0.00	0.00	0.00	0.00	55.4
23	**0.50**	**0.50**	0.02	**0.39**	**1.00**	**0.50**	0.00	0.00	0.00	0.00	0.00	0.00	0.00	0.00	27.0
24	**0.54**	**0.54**	0.02	**0.42**	**1.00**	**0.54**	0.00	0.01	0.00	0.00	0.00	0.00	0.00	0.00	12.4
25	**0.52**	**0.52**	0.02	**0.40**	**1.00**	**0.52**	0.00	0.01	0.00	0.00	0.00	0.00	0.00	0.00	11.2
26	**0.52**	**0.52**	0.02	**0.40**	**1.00**	**0.52**	0.00	0.01	0.00	0.00	0.00	0.00	0.00	0.00	11.1
27	**0.54**	**0.54**	0.02	**0.42**	**1.00**	**0.54**	0.00	0.01	0.00	0.00	0.00	0.00	0.00	0.00	11.4
28	**0.55**	**0.55**	0.02	**0.42**	**1.00**	**0.55**	0.00	0.01	0.00	0.00	0.00	0.00	0.00	0.00	11.6
29	**0.54**	**0.54**	0.02	**0.42**	**1.00**	**0.54**	0.00	0.02	0.01	0.00	0.00	0.00	0.00	0.00	8.48
30	**0.55**	**0.55**	0.02	**0.42**	**1.00**	**0.55**	0.00	0.01	0.00	0.00	0.00	0.00	0.00	0.00	9.12
31	**0.54**	**0.54**	0.02	**0.42**	**1.00**	**0.54**	0.00	0.02	0.00	0.00	0.00	0.00	0.00	0.00	7.86
32	**0.55**	**0.55**	0.02	**0.42**	**1.00**	**0.55**	0.00	0.02	0.00	0.00	0.00	0.00	0.00	0.00	6.35
33	**0.56**	**0.56**	0.02	**0.43**	**1.00**	**0.56**	0.00	0.02	0.00	0.00	0.00	0.00	0.00	0.01	6.83
34	**0.56**	**0.56**	0.02	**0.43**	**1.00**	**0.56**	0.00	0.01	0.00	0.00	0.00	0.00	0.00	0.01	8.87
35	**0.56**	**0.56**	0.01	**0.42**	**1.00**	**0.56**	0.00	0.01	0.00	0.00	0.00	0.00	0.00	0.01	6.56
36	**0.56**	**0.56**	0.01	**0.42**	**1.00**	**0.56**	0.00	0.02	0.00	0.00	0.00	0.00	0.00	0.02	7.85
40	0.00	**0.55**	0.01	**0.44**	**1.00**	**0.55**	0.00	0.04	0.00	0.00	0.00	0.00	0.00	0.00	16.3
41	0.00	**0.55**	0.07	**0.45**	**1.00**	**0.55**	0.01	0.09	0.00	0.00	0.00	0.00	0.00	0.00	15.4
42	0.00	**0.55**	0.01	**0.45**	**1.00**	**0.55**	0.01	0.09	0.00	0.00	0.00	0.00	0.00	0.00	16.2
43	0.00	**0.55**	0.01	**0.45**	**1.00**	**0.55**	0.01	**0.15**	0.00	0.00	0.00	0.00	0.00	0.00	15.6
44	0.00	**0.55**	0.01	**0.45**	**1.00**	**0.55**	0.01	**0.14**	0.00	0.00	0.00	0.00	0.00	0.00	12.8
45	0.00	**0.55**	0.02	**0.45**	**1.00**	**0.55**	0.01	**0.11**	0.00	0.00	0.00	0.00	0.00	0.00	12.1
46	0.00	**0.55**	0.02	**0.45**	**1.00**	**0.55**	0.01	**0.17**	0.00	0.00	0.00	0.00	0.00	0.00	11.0
47	0.00	**0.55**	0.02	**0.45**	**1.00**	**0.55**	0.02	**0.21**	0.00	0.00	0.00	0.00	0.00	0.00	11.0
48	0.00	**0.55**	0.02	**0.45**	**1.00**	**0.55**	0.01	**0.17**	0.00	0.00	0.00	0.00	0.00	0.00	9.99

49	0.00	**0.55**	0.02	**0.44**	**1.00**	**0.55**	0.01	**0.13**	0.00	0.00	0.00	0.00	0.00	0.00	9.22
50	0.00	**0.55**	0.02	**0.44**	**1.00**	**0.55**	0.01	0.08	0.00	0.00	0.00	0.00	0.00	0.00	12.9
51	0.00	**0.55**	0.02	**0.44**	**1.00**	**0.55**	0.01	0.08	0.00	0.00	0.00	0.00	0.00	0.00	10.2
52	0.00	**0.55**	0.02	**0.44**	**1.00**	**0.55**	0.01	**0.12**	0.00	0.00	0.00	0.00	0.00	0.00	10.7
53	0.00	**0.55**	0.02	**0.45**	**1.00**	**0.55**	0.01	**0.18**	0.00	0.00	0.00	0.00	0.00	0.01	8.21
54	0.00	**0.55**	0.02	**0.44**	**1.00**	**0.55**	0.01	0.08	0.00	0.00	0.00	0.00	0.00	0.00	12.5
55	0.00	**0.55**	0.02	**0.45**	**1.00**	**0.55**	0.01	**0.17**	0.00	0.00	0.00	0.00	0.00	0.01	8.80
56	0.00	**0.55**	0.02	**0.45**	**1.00**	**0.55**	0.01	**0.19**	0.00	0.00	0.00	0.00	0.00	0.01	9.67
57	0.00	**0.55**	0.02	**0.44**	**1.00**	**0.55**	0.01	**0.11**	0.00	0.00	0.00	0.00	0.00	0.00	10.4
58	0.00	**0.55**	0.02	**0.44**	**1.00**	**0.55**	0.01	0.07	0.00	0.00	0.00	0.00	0.00	0.00	11.6
59	0.00	**0.55**	0.02	**0.45**	**1.00**	**0.55**	0.01	**0.17**	0.00	0.00	0.00	0.00	0.00	0.01	8.24
60	0.00	**0.56**	0.02	**0.45**	**1.00**	**0.56**	0.01	**0.17**	0.01	0.00	0.00	0.00	0.00	0.01	9.30
61	0.00	**0.56**	0.02	**0.44**	**1.00**	**0.56**	0.01	**0.10**	0.00	0.00	0.00	0.00	0.00	0.01	7.61
62	0.00	**0.56**	0.02	**0.44**	**1.00**	**0.56**	0.00	0.05	0.00	0.00	0.00	0.00	0.00	0.01	12.4

Table 3

The values of the objective function (see eq. (1)) in the various rounds of optimization.

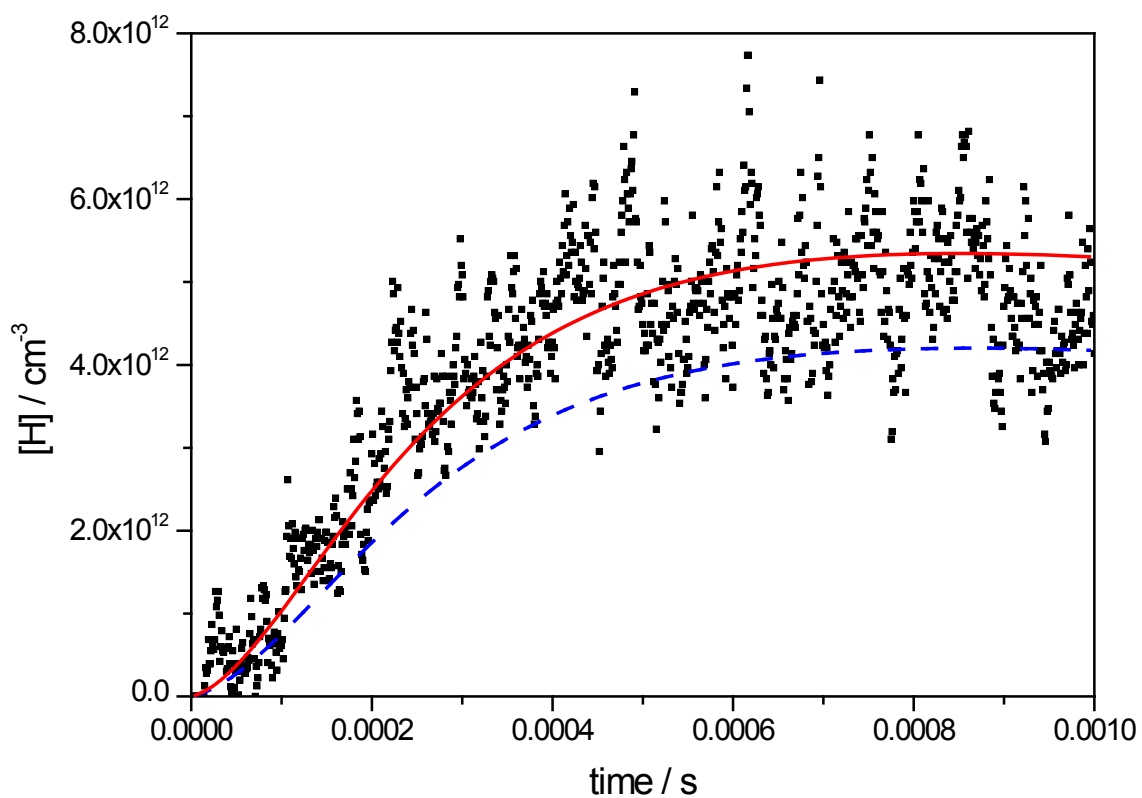| Experimental data considered	Peukert *et al.* mechanism [4]	Initial mechanism	Mechanism after the optimization
Fernandes only [5]	N/A	9.0	9.9
1-hexene only [4]	118.4	220.5	153.4
cyclohexane only [4]	462.9	657.0	325.0
cyclohexane+1-hexene [4]	581.4	877.5	482.4
all experimental data	N/A	886.5	492.3

Fig. 1. Measured H-atom concentrations in one of the 1-hexene experiments (1-C_6H_{12} concentration = 1.3 ppm, p = 1.86 bar, T = 1260 K) and the simulation results using the initial mechanism (blue dashed line) and the final optimized mechanism (red solid line)

Fig. 2. Measured H-atom concentrations in one of the cyclohexane experiments (c-C_6H_{12} concentration = 2.0 ppm, p = 1.68 bar, T = 1462 K) and the simulation results using the initial mechanism (blue dashed line) and the final optimized mechanism (red solid line).
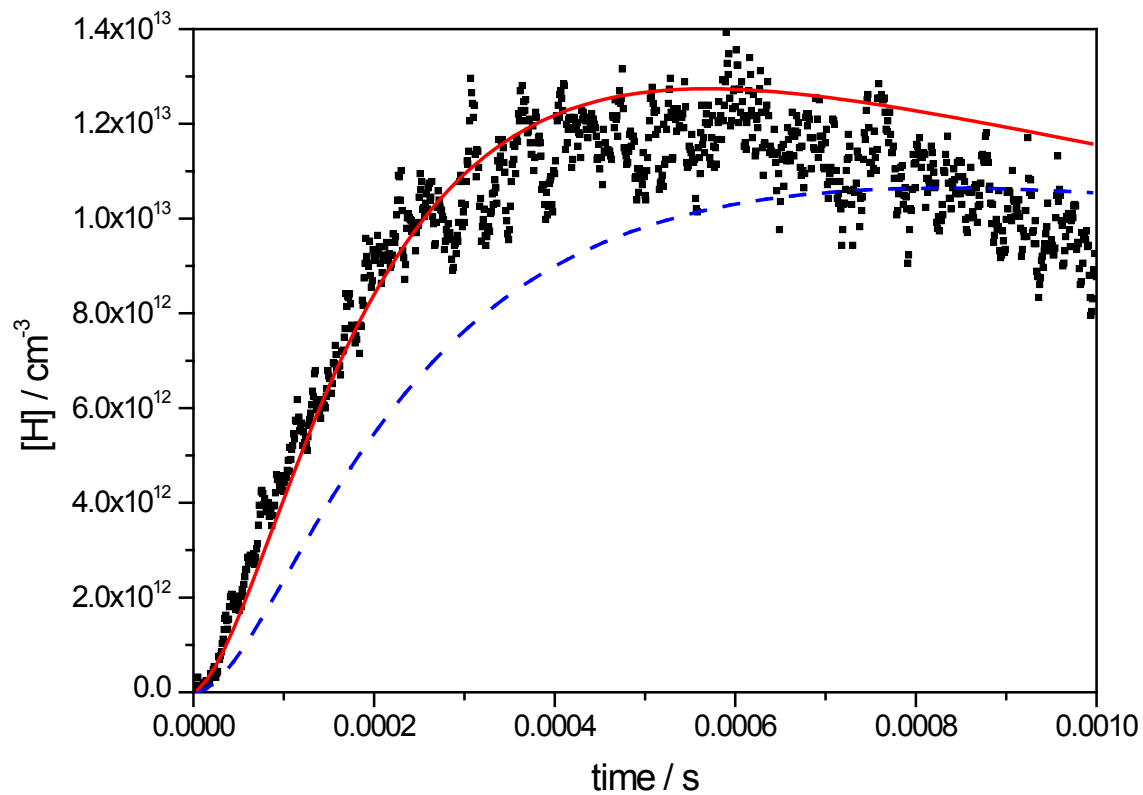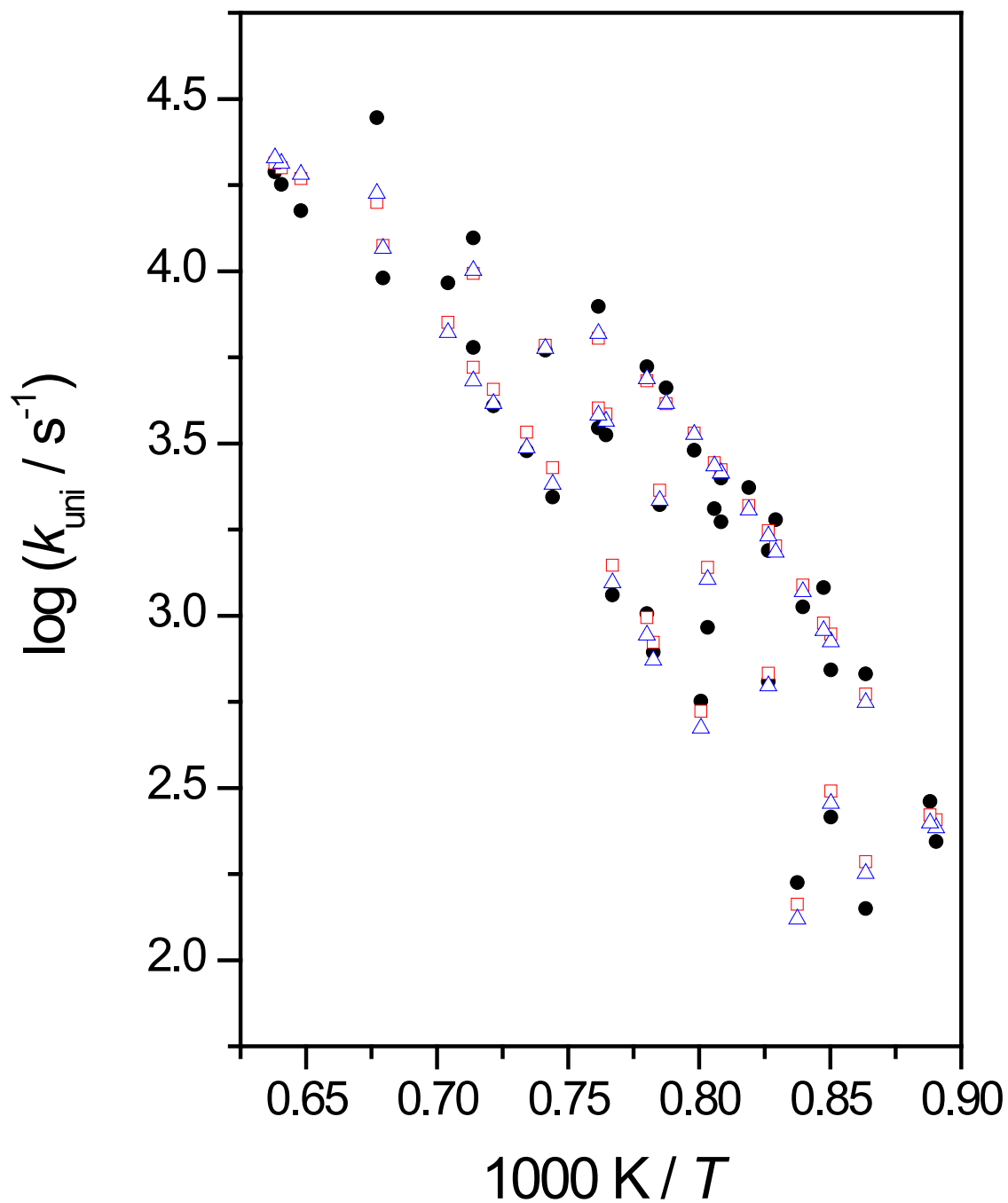
Fig. 3. Results of the Fernandes *et al.* experiments [5] (black full circles) and the calculated k_{uni} values, when the rate parameters of the Lindemann scheme are fitted to these experiments only (blue open triangles) and using the parameters fitted to all experimental data (red open squares).
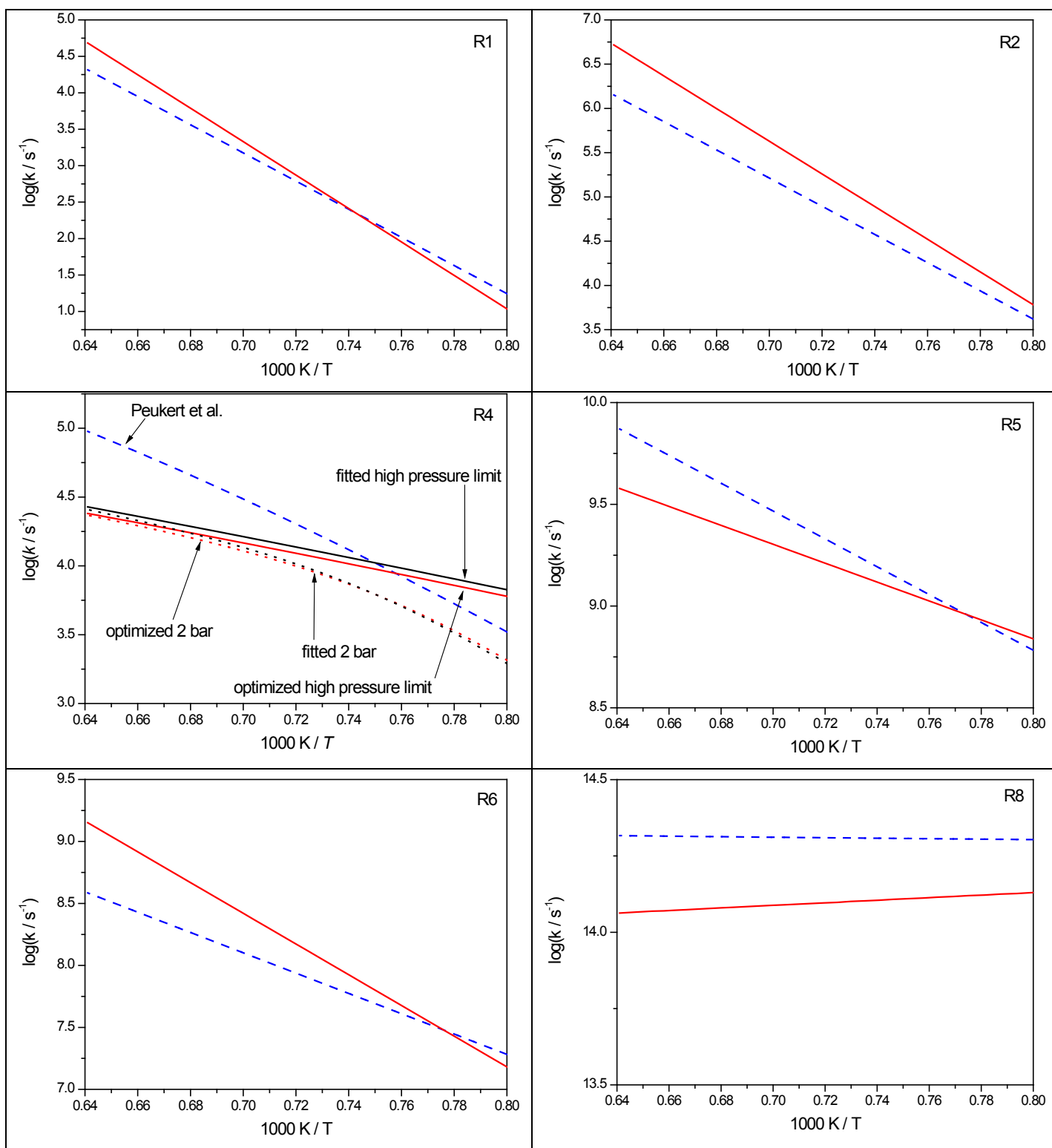
Fig. 4. Arrhenius plots of the rate coefficients investigated in the work. The solid red line is the optimized rate coefficient and the dashed blue line corresponds to the values used by Peukert *et al.* [4]. The figure in panel belonging to R4 contains also the high pressure limit and k_{uni} belonging to 2 bar, as determined from fitting to the Fernandes *et al.* [5] experiments only, and the corresponding functions obtained by the optimization.
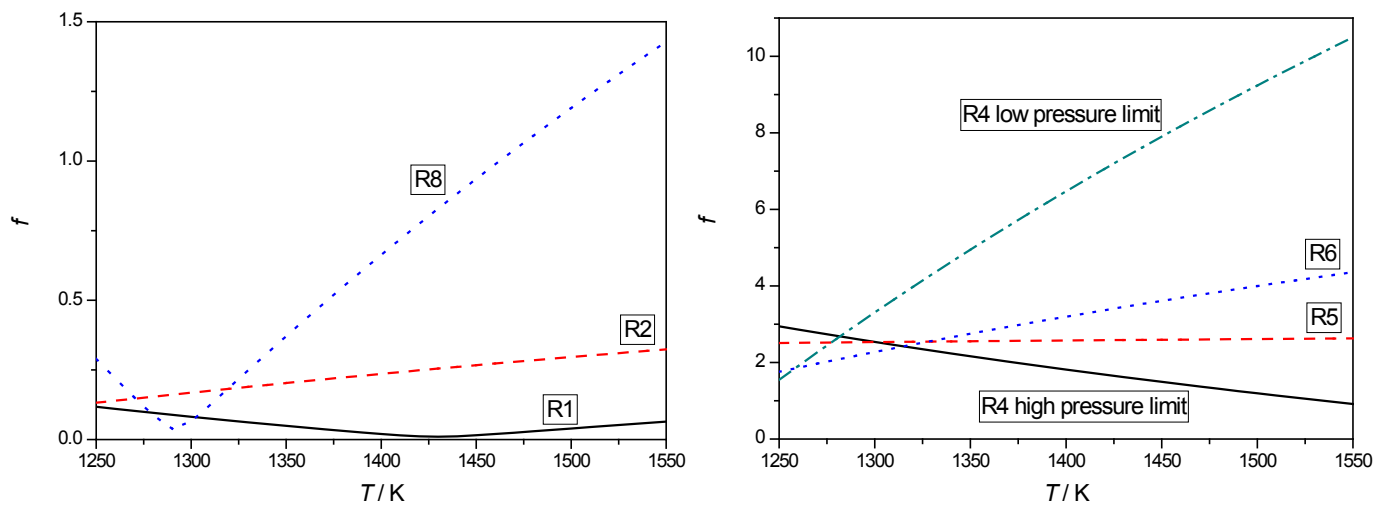
Fig. 5. Uncertainty parameter f as a function of temperature for the optimized reactions in the 1250–1550K temperature interval.

	1	2	3	4	5	6	7	8	9	10	11	12	13	14	15	16
1	3.92160E-01	5.60508E+02	5.57905E-01	6.30281E+02	-6.30371E+00	3.28863E-01	-6.69736E+03	-1.48076E+00	-3.56410E+02	-7.23319E+00	-7.99682E+03	4.05873E+00	5.24090E+03	-5.13134E+00	-2.13311E+00	-2.45109E+04
2	5.60508E+02	8.01250E+05	7.97627E+02	9.01081E+05	-9.01449E+03	4.70005E+02	-9.58108E+06	-2.11788E+03	-5.10092E+05	-1.03455E+04	-1.14381E+07	5.80569E+03	7.49672E+06	-7.34596E+03	-3.05118E+03	-3.50677E+07
3	5.57905E-01	7.97627E+02	8.02173E-01	9.02491E+02	-9.03442E+00	4.72018E-01	-9.59673E+03	-2.12733E+00	-5.14123E+02	-1.03794E+01	-1.14703E+04	5.84897E+00	7.55416E+03	-7.47293E+00	-3.05087E+00	-3.52156E+04
4	6.30281E+02	9.01081E+05	9.02491E+02	1.01895E+06	-1.01699E+04	5.30336E+02	-1.08118E+07	-2.39457E+03	-5.76933E+05	-1.16972E+04	-1.29321E+07	6.56835E+03	8.48189E+06	-8.42815E+03	-3.43228E+03	-3.96465E+07
5	-6.30371E+00	-9.01449E+03	-9.03442E+00	-1.01699E+04	1.03064E+02	-5.41742E+00	1.09066E+05	2.42471E+01	5.94882E+03	1.18140E+02	1.30638E+05	-6.64996E+01	-8.58888E+04	8.44347E+01	3.47150E+01	3.99990E+05
6	3.28863E-01	4.70005E+02	4.72018E-01	5.30336E+02	-5.41742E+00	2.94960E-01	-5.61529E+03	-1.26653E+00	-3.12473E+02	-6.17553E+00	-6.83059E+03	3.48040E+00	4.49602E+03	-4.32326E+00	-1.80214E+00	-2.06906E+04
7	-6.69736E+03	-9.58108E+06	-9.59673E+03	-1.08118E+07	1.09066E+05	-5.61529E+03	1.16786E+08	2.57676E+04	6.30730E+06	1.25493E+05	1.38750E+08	-7.06055E+04	-9.11836E+07	9.06945E+04	3.70213E+04	4.27364E+08
8	-1.48076E+00	-2.11788E+03	-2.12733E+00	-2.39457E+03	2.42471E+01	-1.26653E+00	2.57676E+04	5.77702E+00	1.45856E+03	2.80190E+01	3.09984E+04	-1.57429E+01	-2.03336E+04	1.98800E+01	8.22810E+00	9.46459E+04
9	-3.56410E+02	-5.10092E+05	-5.14123E+02	-5.76933E+05	5.94882E+03	-3.12473E+02	6.30730E+06	1.45856E+03	4.15945E+05	6.94315E+03	7.70081E+06	-3.88883E+03	-5.02498E+06	4.82116E+03	2.03004E+03	2.32484E+07
10	-7.23319E+00	-1.03455E+04	-1.03794E+01	-1.16972E+04	1.18140E+02	-6.17553E+00	1.25493E+05	2.80190E+01	6.94315E+03	1.36452E+02	1.50971E+05	-7.66500E+01	-9.89984E+04	9.69788E+01	4.00595E+01	4.61035E+05
11	-7.99682E+03	-1.14381E+07	-1.14703E+04	-1.29321E+07	1.30638E+05	-6.83059E+03	1.38750E+08	3.09984E+04	7.70081E+06	1.50971E+05	1.67067E+08	-8.47592E+04	-1.09472E+08	1.07213E+05	4.43023E+04	5.09823E+08
12	4.05873E+00	5.80569E+03	5.84897E+00	6.56835E+03	-6.64996E+01	3.48040E+00	-7.06055E+04	-1.57429E+01	-3.88883E+03	-7.66500E+01	-8.47592E+04	4.33077E+01	5.59464E+04	-5.45132E+01	-2.25557E+01	-2.59452E+05
13	5.24090E+03	7.49672E+06	7.55416E+03	8.48189E+06	-8.58888E+04	4.49602E+03	-9.11836E+07	-2.03336E+04	-5.02498E+06	-9.89984E+04	-1.09472E+08	5.59464E+04	7.22750E+07	-7.03965E+04	-2.91334E+04	-3.35095E+08
14	-5.13134E+00	-7.34596E+03	-7.47293E+00	-8.42815E+03	8.44347E+01	-4.32326E+00	9.06945E+04	1.98800E+01	4.82116E+03	9.69788E+01	1.07213E+05	-5.45132E+01	-7.03965E+04	8.32674E+01	2.72016E+01	3.34153E+05
15	-2.13311E+00	-3.05118E+03	-3.05087E+00	-3.43228E+03	3.47150E+01	-1.80214E+00	3.70213E+04	8.22810E+00	2.03004E+03	4.00595E+01	4.43023E+04	-2.25557E+01	-2.91334E+04	2.72016E+01	1.19737E+01	1.35640E+05
16	-2.45109E+04	-3.50677E+07	-3.52156E+04	-3.96465E+07	3.99990E+05	-2.06906E+04	4.27364E+08	9.46459E+04	2.32484E+07	4.61035E+05	5.09823E+08	-2.59452E+05	-3.35095E+08	3.34153E+05	1.35640E+05	1.56806E+09

Table S1. The covariance matrix of the parameters. The order of the optimized parameters is R1: *A, E/R*; R2: *A, E/R*; R4(high pressure limit): *A, n, E/R*; R4(low pressure limit): *A, n, E/R*; R5: *A, E/R*; R6: *A, E/R*; R8: *A, E/R*.

	1	2	3	4	5	6	7	8	9	10	11	12	13	14	15	16
1	1.00000E+00	9.99923E-01	9.94705E-01	9.97071E-01	-9.91544E-01	9.66944E-01	-9.89640E-01	-9.83788E-01	-8.82471E-01	-9.88799E-01	-9.87963E-01	9.84865E-01	9.84419E-01	-8.97970E-01	-9.84391E-01	-9.88433E-01
2	9.99923E-01	1.00000E+00	9.94905E-01	9.97248E-01	-9.91983E-01	9.66800E-01	-9.90456E-01	-9.84386E-01	-8.83581E-01	-9.89410E-01	-9.88613E-01	9.85571E-01	9.85130E-01	-8.99347E-01	-9.85078E-01	-9.89332E-01
3	9.94705E-01	9.94905E-01	1.00000E+00	9.98234E-01	-9.93604E-01	9.70382E-01	-9.91502E-01	-9.88208E-01	-8.90051E-01	-9.92086E-01	-9.90819E-01	9.92346E-01	9.92106E-01	-9.14364E-01	-9.84409E-01	-9.92934E-01
4	9.97071E-01	9.97248E-01	9.98234E-01	1.00000E+00	-9.92400E-01	9.67371E-01	-9.91118E-01	-9.86961E-01	-8.86197E-01	-9.92007E-01	-9.91169E-01	9.88774E-01	9.88376E-01	-9.14993E-01	-9.82637E-01	-9.91853E-01
5	-9.91544E-01	-9.91983E-01	-9.93604E-01	-9.92400E-01	1.00000E+00	-9.82556E-01	9.94121E-01	9.93701E-01	9.08573E-01	9.96218E-01	9.95567E-01	-9.95368E-01	-9.95152E-01	9.11445E-01	9.88214E-01	9.94982E-01
6	9.66944E-01	9.66800E-01	9.70382E-01	9.67371E-01	-9.82556E-01	1.00000E+00	-9.56743E-01	-9.70248E-01	-8.92097E-01	-9.73425E-01	-9.73042E-01	9.73788E-01	9.73762E-01	-8.72353E-01	-9.58946E-01	-9.62080E-01
7	-9.89640E-01	-9.90456E-01	-9.91502E-01	-9.91118E-01	9.94121E-01	-9.56743E-01	1.00000E+00	9.92035E-01	9.04962E-01	9.94108E-01	9.93328E-01	-9.92798E-01	-9.92493E-01	9.19704E-01	9.90018E-01	9.98669E-01
8	-9.83788E-01	-9.84386E-01	-9.88208E-01	-9.86961E-01	9.93701E-01	-9.70248E-01	9.92035E-01	1.00000E+00	9.40925E-01	9.97953E-01	9.97798E-01	-9.95294E-01	-9.95102E-01	9.06416E-01	9.89313E-01	9.94417E-01
9	-8.82471E-01	-8.83581E-01	-8.90051E-01	-8.86197E-01	9.08573E-01	-8.92097E-01	9.04962E-01	9.40925E-01	1.00000E+00	9.21611E-01	9.23790E-01	-9.16260E-01	-9.16478E-01	8.19210E-01	9.09648E-01	9.10321E-01
10	-9.88799E-01	-9.89410E-01	-9.92086E-01	-9.92007E-01	9.96218E-01	-9.73425E-01	9.94108E-01	9.97953E-01	9.21611E-01	1.00000E+00	9.99903E-01	-9.97101E-01	-9.96882E-01	9.09806E-01	9.91065E-01	9.96695E-01
11	-9.87963E-01	-9.88613E-01	-9.90819E-01	-9.91169E-01	9.95567E-01	-9.73042E-01	9.93328E-01	9.97798E-01	9.23790E-01	9.99903E-01	1.00000E+00	-9.96458E-01	-9.96244E-01	9.09005E-01	9.90529E-01	9.96078E-01
12	9.84865E-01	9.85571E-01	9.92346E-01	9.88774E-01	-9.95368E-01	9.73788E-01	-9.92798E-01	-9.95294E-01	-9.16260E-01	-9.97101E-01	-9.96458E-01	1.00000E+00	9.99991E-01	-9.07782E-01	-9.90511E-01	-9.95618E-01
13	9.84419E-01	9.85130E-01	9.92106E-01	9.88376E-01	-9.95152E-01	9.73762E-01	-9.92493E-01	-9.95102E-01	-9.16478E-01	-9.96882E-01	-9.96244E-01	9.99991E-01	1.00000E+00	-9.07443E-01	-9.90337E-01	-9.95388E-01
14	-8.97970E-01	-8.99347E-01	-9.14364E-01	-9.14993E-01	9.11445E-01	-8.72353E-01	9.19704E-01	9.06416E-01	8.19210E-01	9.09806E-01	9.09005E-01	-9.07782E-01	-9.07443E-01	1.00000E+00	8.61476E-01	9.24756E-01
15	-9.84391E-01	-9.85078E-01	-9.84409E-01	-9.82637E-01	9.88214E-01	-9.58946E-01	9.90018E-01	9.89313E-01	9.09648E-01	9.91065E-01	9.90529E-01	-9.90511E-01	-9.90337E-01	8.61476E-01	1.00000E+00	9.89901E-01
16	-9.88433E-01	-9.89332E-01	-9.92934E-01	-9.91853E-01	9.94982E-01	-9.62080E-01	9.98669E-01	9.94417E-01	9.10321E-01	9.96695E-01	9.96078E-01	-9.95618E-01	-9.95388E-01	9.24756E-01	9.89901E-01	1.00000E+00

Table S2. The correlation matrix of the parameters. The order of the optimized parameters is R1: *A, E/R*; R2: *A, E/R*; R4(high pressure limit): *A, n, E/R*; R4(low pressure limit): *A, n, E/R*; R5: *A, E/R*; R6: *A, E/R*; R8: *A, E/R*.